

UC Berkeley

SEMM Reports Series

Title

Effective Shear Modulus of Honeycomb Cellular Structure

Permalink

<https://escholarship.org/uc/item/3077c87m>

Authors

Penzien, Joseph

Didriksson, Theodor

Publication Date

1963-03-01

500
C23
63/1

SmS

Report No.
SESM-63-1

STRUCTURES AND MATERIALS RESEARCH
DEPARTMENT OF CIVIL ENGINEERING

EFFECTIVE SHEAR MODULUS OF HONEYCOMB CELLULAR STRUCTURE

BY
JOSEPH PENZIEN
THEODOR DIDRIKSSON

UNIVERSITY OF CALIFORNIA
Earthquake Engineering
Research Center

MAR 29 1996

MARCH 1963

LIBRARY
INSTITUTE OF ENGINEERING RESEARCH
UNIVERSITY OF CALIFORNIA
BERKELEY CALIFORNIA

Effective Shear Modulus of Honeycomb Cellular Structure

by

Joseph Penzien
Theodor Didriksson

University of California

March 1963

Foreword

The research described in this report, "Effective Shear Modulus of Honeycomb Cellular Structure" was conducted under the supervision and technical guidance of Joseph Penzien, Professor of Civil Engineering, Division of Structural Engineering and Structural Mechanics, College of Engineering, University of California, Berkeley, California. Mr. Theodor Didriksson, a Graduate Student, carried out the details of the analysis.

Financial support for the program was given by Hexcell Products, Inc. and administered through the Institute of Engineering Research.

Acknowledgement

The authors wish to express their appreciation and sincere thanks to those individuals who contributed to this investigation, especially to Mr. Conway Chan, Graduate Student, who designed the test farms and carried out the experimental tests, to Mr. C. C. Tung, Graduate Student, who reduced the final test data and checked the theoretical derivations, to Mrs. L. Umsted for typing this report, and to Mr. M. I, Kazimi of Hexcell Products, Inc. for his advise and encouragement.

Finally, the authors wish to thank the Hexcell Products, Inc. for their financial support which made this investigation possible.

Notation

The symbols used in this report are defined in the text where they are first introduced. For convenience, they are summarized here in alphabetical order.

a, b	= dimension of typical element of core shown in Figure 1
d	= thickness of the members of the shear loading frame; refer to Figure 8
E_{ξ} , E_{γ}	= moduli of elasticity of the core element ABCD in the ξ and γ directions, respectively; refer to Equations (13) and (14)
E	= E_{γ}
F	= area of typical element of core as defined by Equation (2)
f_1	= d/L_1
f_2	= d/L_2
G	= shear modulus of the core material
G_c	= effective shear modulus of the honeycomb cellular material as defined by Equation (1); refer also to Equation (53)
H	= $\frac{1}{2}(a + b)$
K_1 , K_2	= loading frame coefficients as defined by Equations (46) and (52)
K_3	= quantity defined by Equation (50)
L	= depth of the core; refer to Figure 1
L_1 , L_2	= dimensions of the shear loading frame; refer to Figure 8
M_1 , M_4 , M_5 , M_8	= frictional moments developed at the joints of the shear loading frame; refer to Figure 8

- P = diagonal loads applied to the shear loading frame; refer to Figure 8
- p, q = shear flows in the typical core element induced by the shear forces V_y and V_x , respectively
- Q, Q' = shear forces between the core and the shear loading frame; refer to Figure 8
- R = b/a
- r = radius of the shear loading frame holes
- S = dimensionless quantity defined by Equation (35)
- s = width of the core; refer to Figure 8
- T = dimensionless quantity defined by Equation (36)
- t = thickness of the core material; refer to Figure 1
- u, v = displacement components of the typical element ABCD in the ξ and γ directions, respectively; refer to Equations (13) and (14)
- V = shear force applied on the faces of the typical element of core; refer to Figure 2
- V_x, V_y = components of V in the x and y directions, respectively; refer to Figures 3 and 5
- w = warpage parameter defined by Equation (10)
- α = angle of inclination of the load P applied to the shear loading frame; refer to Figure 8
- γ = overall shear strain of the typical element of the core
- γ_x, γ_y = components of γ in the x and y directions, respectively
- $\delta_{\xi\gamma}$ = shear strain in element ABCD; refer to Equation (15)
- δ_1, δ_2 = shear strains arising in the unrestrained typical element of the core under the shearing forces V_x ; refer to Figure 3b

- Δ = relative shear displacement vector of the typical element of core; refer to Figure 2
- Δ_x, Δ_y = components of Δ in the x and y directions, respectively
- $\epsilon_\xi, \epsilon_\zeta$ = normal strain components of the typical element ABCD in the ξ and ζ directions, respectively; refer to Equations (13) and (14)
- θ = geometrical quantity of the typical core element; refer to Figure 1
- μ = coefficient of sliding friction between the pins and the shear loading frame holes
- μ_ξ, μ_ζ = Poisson's coefficients of the typical element ABCD in the ξ and ζ directions, respectively; refer to Equations (13) and (14)
- ρ, ρ_c = densities of the core material and the core, respectively; refer to Equation (54)
- σ_ξ, σ_ζ = normal stress components of the typical element ABCD in the ξ and ζ directions, respectively
- $\tau_{\xi\zeta}$ = shearing stress in the typical element ABCD
- ϕ, ψ = angles specifying the directions of the shear force V, and the relative shear displacement Δ , respectively; refer to Figure 1

I. Introduction

Honeycomb cellular materials are now widely used in the aircraft and missile industry because of their high strength to mass ratios. Usually these materials are bonded between flat or curved surfaces to form integral parts of load carrying structural elements.

Due to their characteristic geometry, honeycomb cellular materials are especially effective in transmitting shear loads. When carrying such loads, the amounts of shear deformation produced may be important design criteria; therefore, it is important that design engineers be able to predict these deformations analytically. To make these predictions, however, the effective shear moduli of these honeycomb cellular materials must be known. While both analytical and experimental methods have been used to predict effective shear moduli, considerable reluctance has been expressed by some engineers to accept these values as being sufficiently accurate. This reluctance is understandable when one observes the large variations in moduli which have been measured experimentally by several methods and the poor correlations which appear to exist in some instances with theory.

It is the purpose of this report to set forth a sufficiently accurate theory for predicting effective shear moduli of honeycomb cellular materials and also to suggest an effective test procedure for measuring these quantities. A correlation of experimental results obtained by this suggested procedure with the theory presented herein is also included.

II. Theoretical Analysis

The honeycomb cellular (or core) material analyzed in this report has a cross-section as shown in Figure 1. To determine the effective shear modulus of this material, consider the basic element of which

it is made as shown in Figure 2. A shear force resultant V is applied to both the upper and lower faces of this element in opposite directions and at an angle ϕ with the longitudinal or x axis. The direction of the resulting relative shear displacement vector Δ of the faces of the element does not, in general, coincide with the direction of the applied shear forces. If one defines an angle ψ as the angle between the shear displacement vector Δ and the longitudinal axis, then an effective shear modulus may be defined as

$$G_c \equiv \frac{V}{F \delta \cos(\phi - \psi)} \quad (1)$$

where

$$F \equiv 2(b + a \cos \theta) a \sin \theta \quad (2)$$

is the rectangular area enclosing the typical element and $\delta \equiv \frac{\Delta}{L}$ is the overall shear strain of the element due to the applied shear force V ; L being the depth of the core. It is evident from geometrical considerations that the component of the applied shear force in the transverse (longitudinal) direction does not produce shear displacement in the longitudinal (transverse) direction. Therefore, one may determine the relation between V_x and δ_x ($\equiv \frac{\Delta_x}{L}$) and the relation between V_y and δ_y ($\equiv \frac{\Delta_y}{L}$) separately. Here Δ_x and Δ_y represent the components of Δ in the longitudinal and transverse directions, respectively; thus, the total shear strain δ is given by

$$\delta = \sqrt{\delta_x^2 + \delta_y^2} \quad (3)$$

and the direction of the shear displacement by

$$\psi = \tan^{-1} \frac{\delta_y}{\delta_x} \quad (4)$$

To obtain the relation between V_x and δ_x , consider the typical element as shown in Figure 3a, which is subjected to a uniform shear flow q . To satisfy the equilibrium condition in the vertical (z) direction at each corner of the cell, the shear flow in each panel must, of course, be equal. Figure 3b is an elevation view of the element showing the shear strain in each panel.

It is readily seen that

$$\delta_1 = \frac{q}{Gt} \quad (5)$$

$$\delta_2 = \frac{q a (1 - \cos \theta)}{Gt (b + a \cos \theta)} \quad (6)$$

where G is the shear modulus of the core material. The overall shear strain δ_x is

$$\delta_x = \delta_1 + \delta_2 = \frac{q}{Gt} \frac{2H}{a(R + \cos \theta)} \quad (7)$$

where

$$R = \frac{b}{a} \quad (8)$$

and

$$H = \frac{1}{2} (a + b) \quad (9)$$

Under this loading condition, it is apparent that warping occurs at the upper and lower faces of the core element. The warpage parameter w is defined as

$$w = \frac{b}{2} \delta_2 = \frac{qb (1 - \cos \theta)}{2 Gt (R + \cos \theta)} \quad (10)$$

However, in most practical cases, as well as in the experiment which will be described in the subsequent section, the faces of the core are constrained so that they remain essentially plane during deformation; that is, the actual configuration of the deformed core element is as shown by the dashed lines in Figure 3b.

To study the effect which the constraint against warpage of the faces has on the shear modulus of the core, consider the element ABCD in Figure 3b. One must now find the corrective state of stress in this element when subjected to the displacement boundary conditions that the vertical edges AD and BC are simply supported and the upper and lower edges AB and CD are subjected to vertical displacements equal in magnitude but opposite in direction to the warpage indicated in Figure 3b. Several simplifications and assumptions are made in the following analysis. First, the inclined panel I is unfolded into the plane of panel II. Second, it is assumed that the amount of stretching of the panels in the direction perpendicular to the direction of the essential normal stresses is negligible. Consequently, one may consider the panels as composed of an orthotropic material which is rigid in one direction. Third, the thickness t of the panels is so small compared with other dimensions that one can consider the state of stress in the panels as being plane stress. The typical element ABCD is again shown in Figure 4.

The equations of equilibrium for element ABCD are given by

$$\frac{\partial \sigma_{\xi}}{\partial \xi} + \frac{\partial \tau_{\xi\eta}}{\partial \eta} = 0 \quad (11)$$

and

$$\frac{\partial \tau_{\xi\eta}}{\partial \xi} + \frac{\partial \sigma_{\eta}}{\partial \eta} = 0 \quad (12)$$

The stress-strain relationships are

$$\epsilon_{\xi} = \frac{\partial u}{\partial \xi} = \frac{1}{E_{\xi}} (\sigma_{\xi} - \mu_{\xi} \sigma_{\eta}) \quad (13)$$

$$\epsilon_{\eta} = \frac{\partial v}{\partial \eta} = \frac{1}{E_{\eta}} (\sigma_{\eta} - \mu_{\eta} \sigma_{\xi}) \quad (14)$$

and

$$\delta_{\xi\eta} = \frac{\partial u}{\partial \eta} + \frac{\partial v}{\partial \xi} = \frac{1}{G} \tau_{\xi\eta} \quad (15)$$

In these equations σ_{ξ} , σ_{η} , $\tau_{\xi\eta}$ and ϵ_{ξ} , ϵ_{η} , $\delta_{\xi\eta}$ are the stress and strain components, respectively, and u , v are the displacement components in the ξ and η directions, respectively. The terms E_{ξ} , E_{η} and μ_{ξ} , μ_{η} are the moduli of elasticity and Poisson's ratios of the core material in the ξ and η directions, respectively. For a plate which is rigid in one direction,

$$E_{\xi} = \infty \quad (16)$$

and

$$\mu_{\eta} = 0 \quad (17)$$

Thus, Equation (13) becomes

$$\frac{\partial u}{\partial \xi} = 0 \quad (18)$$

and u is a function of the variables η only; that is $u = u(\eta)$.

If E is written for E_{η} , Equations (14) and (15) take the form

$$E \frac{\partial v}{\partial \eta} = \sigma_{\eta} \quad (19)$$

$$G \frac{\partial v}{\partial \xi} = \tau_{\xi\eta} - u'(\eta) G \quad (20)$$

Differentiating Equations (19) and (20) with respect to η and ξ , respectively, and substituting into Equation (12), one obtains

$$G \frac{\partial^2 v}{\partial \xi^2} + E \frac{\partial^2 v}{\partial \eta^2} = 0 \quad (21)$$

The boundary conditions are

$$\begin{aligned} v(0, \eta) = v(H, \eta) = 0 \\ v(\xi, 0) = v(\xi, L) = \begin{cases} \frac{2w}{b} \xi & ; 0 \leq \xi \leq \frac{b}{2} \\ \frac{2w}{a} (H - \xi) & ; \frac{b}{2} \leq \xi \leq H \end{cases} \end{aligned} \quad (22)$$

The solution of the partial differential Equation (21) with boundary conditions (22) may be obtained by Fourier's method. The final solution, which results by this method is

$$v = \sum_{n=1}^{\infty} \beta_n \sin \frac{n\pi}{H} \xi \frac{1}{\sinh g_n L} \left[\sinh g_n (L-\gamma) + \sinh g_n \gamma \right] \quad (23)$$

where

$$g_n^2 = \frac{G}{E} \left(\frac{n\pi}{H} \right)^2 = \frac{1}{2(1 + \mu\gamma)} \left(\frac{n\pi}{H} \right)^2 \quad (24)$$

and

$$\beta_n = \frac{2}{H} \left[\int_0^{\frac{b}{2}} \frac{2w}{b} \xi \sin \frac{n\pi}{H} \xi d\xi + \int_{\frac{b}{2}}^H \frac{2w}{a} (H - \xi) \sin \frac{n\pi}{H} \xi d\xi \right] \quad (25)$$

Substituting Equation (10) into Equation (25) and integrating, one obtains

$$\beta_n = \frac{4q}{Gta} \frac{(1 - \cos \theta)}{(R + \cos \theta)} \frac{\sin (n\pi \frac{R}{1+R})}{(\frac{n\pi}{H})^2} \quad (26)$$

The normal stresses in the panels may now be obtained from Equation (19); thus

$$\sigma_\gamma = E \frac{\partial v}{\partial \gamma} = E \sum_{n=1}^{\infty} \frac{\beta_n g_n \sin (\frac{n\pi}{H} \xi)}{\sinh g_n L} \left[\cosh g_n \gamma - \cosh g_n (L - \gamma) \right] \quad (27)$$

The shear stresses are similarly obtained from Equation (20). Equation (18) shows that u is independent of ξ ; that is, $u = u(\gamma)$, and therefore since $u(\gamma) = 0$ at both $\xi = 0$ and $\xi = H$, $u(\gamma) = 0$ throughout the panel. Hence, Equation (20) gives

$$\tau_{\xi\gamma} = G \frac{\partial v}{\partial \xi} = G \sum_{n=1}^{\infty} \frac{\beta_n \frac{n\pi}{H} \cos (\frac{n\pi}{H} \xi)}{\sinh g_n L} \left[\sinh g_n (L-\gamma) + \sinh g_n \gamma \right] \quad (28)$$

The total shear stresses and the normal stresses in the unwarped deformed element ABCD in Figure 3b are

$$\tau = \frac{q}{t} + \tau_{\xi\gamma} \quad (29)$$

and

$$\sigma = \sigma_{\gamma} \quad (30)$$

The corresponding shear forces V_x may now be evaluated by energy considerations. The total external work is

$$\text{External work} = \frac{1}{2} \delta_x L \frac{V_x}{4} \quad (31)$$

where δ_x is the overall shear strain given by Equation (7).

The total strain energy is

$$\text{Strain energy} = \int \frac{\tau^2}{2G} d\lambda + \int \frac{\sigma^2}{2E} d\lambda \quad (32)$$

where $d\lambda$ is the differential volume of the element under consideration and the integration extends over the entire volume of the element ABCD. Substituting Equations (7), (27), (28), (29), and (30) into the energy Equation (33)

$$\frac{1}{2} \delta_x L \frac{V_x}{4} = \int \frac{\tau^2}{2G} d\lambda + \int \frac{\sigma^2}{2E} d\lambda \quad (33)$$

gives after integrating and rearranging the following expression for the shear V_x

$$V_x = 2 q a (R + \cos \theta)(1 + ST) \quad (34)$$

where

$$S = \frac{2(1 - \cos \theta)^2 (1 + R)^2 \sqrt{2(1 + \mu_r)}}{\frac{L}{H} \pi^3 (R + \cos \theta)^2} \quad (35)$$

and

$$T = \frac{1}{n^3} \left(\frac{\sin \frac{n\pi R}{1+R}}{\sinh g_n L} \right)^2 (\sinh 2g_n L - 2 \sinh g_n L) \quad (36)$$

Eliminating q from Equations (7) and (34) gives

$$\gamma_x = \frac{HV \cos \phi}{Gt a^2 (R + \cos \theta)^2 (1 + ST)} \quad (37)$$

where $V \cos \phi = V_x$. The term ST is due to the prevention of warpage.

To determine the relation between V_y and γ_y consider the typical element acted upon by the shear flows p as indicated in Figure 5. It is evident from geometrical considerations that there will be no warping. The overall shear strain in

$$\gamma_y = \frac{p}{Gt \sin \theta} \quad (38)$$

and the shear force V_y is

$$V_y = 2pa \sin \theta \quad (39)$$

Eliminating p from Equations (38) and (39) gives the following relation between γ_y and V_y .

$$\gamma_y = \frac{V \sin \phi}{2a Gt \sin^2 \theta} \quad (40)$$

where

$$V \sin \phi = V_y$$

The effect of preventing warpage upon the value of the shear modulus of the core is now studied for the particular case where $\phi = 0$, $R = 1$, $\theta = 60^\circ$ and $\mu_z = 0.33$. The final result of this study is shown in Figure 6. It is seen that for moderately large values of $\frac{L}{H}$ the effect of the prevention of warpage may be ignored. In such

cases, Equation (37) reduces to

$$\gamma_x = \frac{H V \cos \phi}{Gt a^2 (R + \cos \theta)^2} \quad (41)$$

Equation (41) together with Equation (40) gives

$$\gamma = \frac{V}{Gta} \left[\frac{H^2 \cos^2 \phi}{a^2 (R + \cos \theta)^4} + \frac{\sin^2 \phi}{4 \sin^4 \theta} \right]^{1/2} \quad (42)$$

and

$$\cos (\phi - \psi) = \left[\frac{\sin^2 \phi}{2 \sin^2 \theta} + \frac{H \cos^2 \phi}{a(R + \cos \theta)^2} \right] \left[\frac{H^2 \cos^2 \phi}{a^2 (R + \cos \theta)^4} + \frac{\sin^2 \phi}{4 \sin^4 \theta} \right]^{-1/2} \quad (43)$$

Substituting these expressions into Equation (1), gives

$$\frac{G_c}{G} = \frac{\sin \theta (R + \cos \theta)}{\frac{a}{t} \left[(1+R) \sin^2 \theta \cos^2 \phi + (R + \cos \theta)^2 \sin^2 \phi \right]} \quad (44)$$

III. Experimental Investigation

To induce pure shear in the core, a rigid frame pinned at the corners with the honeycomb core bonded within the frame on all four sides was designed, see Figure 7. A tensile load with its line of action through the diagonal of the frame was applied. The relative displacement Δ of the upper and lower faces of the frame was measured by a transducer attached to the lower member of the frame and a rod which was rigidly attached to the upper member and extended down to the transducer. The load and corresponding relative displacement were recorded graphically as the load was increased. Three series of tests were performed on the Hexcell Aluminum Honeycomb-Alloy 5052-H39, Al 1/8-5052, 0.0007P with core depth of 4, 5, and 6 inches. All test specimens were loaded in the longitudinal direction. To deduce the shear modulus of one of these cores from the test results, consider the loading frame shown in Figure 8.

Acting on the frame are the externally applied forces P and the interacting shear forces Q and Q' between the core and the frame where $Q' = Q \left(\frac{L_2 - d}{L_1 - d} \right)$ by consideration of the equilibrium condition of the core. The relation between the shear force V and the applied force P can be deduced easily by applying the principle of virtual work on the equilibrium of the frame shown in Figure 8. Whereby, one gets

$$Q = K_1 P \cos \alpha \quad (45)$$

where

$$K_1 = \frac{1 - f_1}{1 - f_1 f_2} \quad (46)$$

and where

$$f_1 = \frac{d}{L_1}; \quad f_2 = \frac{d}{L_2} \quad (47)$$

During the tests, frictional forces were observed to develop at the joints between the frame holes and the pins--notably at the joints where the loads P were applied. From static considerations, it can be shown easily that the forces at joints A₁ and A₃ (Fig. 8) are small compared to those at joints A₂ and A₄ where the forces P are applied, and the resultant frictional moments at joints A₂ and A₄ may be approximated by

$$M_1 = M_5 = \frac{\mu r}{2} (1 + K_1) \quad (48)$$

$$M_4 = M_8 = \frac{\mu r}{2} \frac{L_2}{L_1} (1 + K_3) \quad (49)$$

where

$$K_3 = \frac{1 - f_2}{1 - f_1 f_2}, \quad (50)$$

r is the radius of the frame holes and μ is the coefficient of sliding friction between the pins and the holes. Again, by means of the principle of virtual work, one obtains

$$Q = K_2 P \cos \alpha \quad (51)$$

where

$$K_2 = K_1 \left[1 - \frac{\mu r}{L_1} (1 + K_3) \right] \quad (52)$$

If the pins and frame holes were well lubricated so that the coefficient of friction μ could be greatly reduced, then K_2 could be approximated by K_1 .

The measured shear moduli of the cores is deduced from the experimental data by the expression

$$G_c = \frac{Q}{\Delta s} \frac{L_2 - d}{L_1 - d} = \frac{P K_1 \cos \alpha}{\Delta s} \frac{L_2}{L_1} \frac{1 - f_2}{1 - f_1} \quad (53)$$

where s is the width of the core and i assumes a value of one or two depending on whether the lubrication problem is properly taken care of or not.

IV. Comparison of Experimental and Theoretical Shear Moduli

Since all tests were performed on cores whose depths L compared to the lateral dimensions H of the cells are large, the effect of warpage may be neglected and Equation (44) may be used for the determination of the theoretical shear moduli of the cores. Introducing now the density of the honeycomb

$$\rho_c = \frac{(1 + R)}{\frac{a}{t} (R + \cos \theta) \sin \theta} \rho \quad (54)$$

where ρ_c and ρ are the densities of the core and the foil material, respectively, Equation (44) reduces to

$$\frac{G_c}{G} \frac{\rho}{\rho_c} = \frac{(R + \cos \theta)^2 \sin^2 \theta}{(1+R) \left[(1+R) \sin^2 \theta \cos^2 \phi + (R + \cos \theta)^2 \sin^2 \phi \right]} \quad (55)$$

Since, in the experiments the load P was applied in the longitudinal direction, i.e., $\phi = 0$, Equation (55) becomes

$$\frac{G_c}{G} \frac{\rho}{\rho_c} = \frac{(R + \cos \theta)^2}{(1+R)^2} \quad (56)$$

Using Equations (53) and (56) it is found that the ratio of the experimental effective shear moduli of the cores to their respective theoretical values ranges approximately from 1.04 to 1.10 when the effect of friction forces at the joints are not taken into consideration. When the friction forces are considered and a value $\mu = 0.25$ is used, this same ratio ranges from 1.04 to 1.06.

V. Conclusions

Based on the results of this investigation, the following general conclusions have been deduced:

- (1) The effective shear modulus of typical honeycomb cores can be determined with sufficient accuracy for design purposes using the theory presented in this report.
- (2) The prevention of warpage of the core cross section has only a small effect on the effective shear modulus when the ratio of the depth of core L to the lateral dimension H of the cell is large; e.g. a 1 percent change results when L/R is approximately 7 (see Figure 6).
- (3) The effective shear modulus of honeycomb cores can be measured effectively using the "shear frame" test described herein. The variations in moduli measured for a given core material by this method are within a range which would be expected as a result of the variations in the geometrical quantities from one sample to another and due to the variations in the shear moduli of the core material itself.

References

1. Kelsey, S., R. A. Gellatly, and B. W. Clark, "Shear Modulus of Foil Honeycomb Cores", Aircraft Engineering, Vol. XXX, October, 1958.
2. Chan, C., "Shear Modulus of Sandwich Cores", M. S. Research Report, University of California, Berkeley, California, 1962.

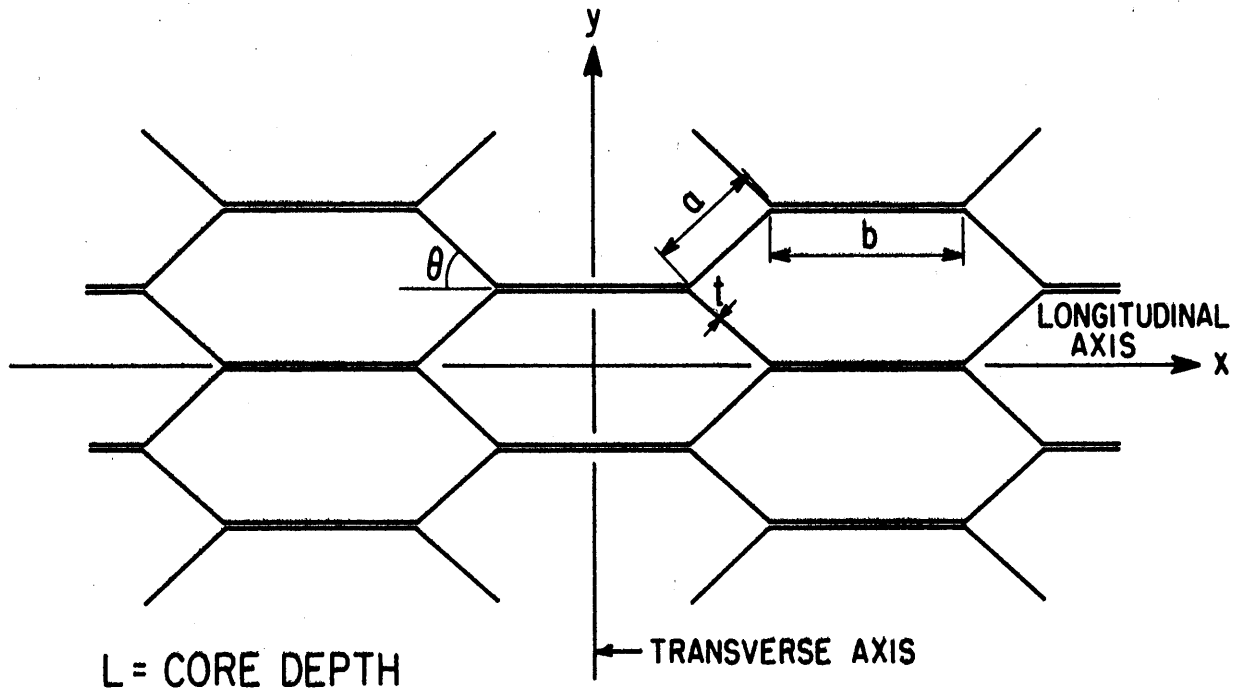


FIG. 1 GEOMETRY OF HONEYCOMB CELLS

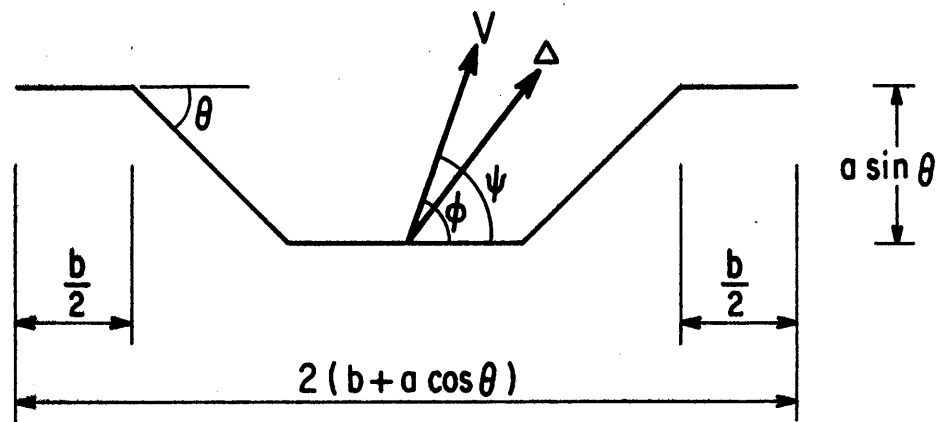


FIG. 2 TYPICAL ELEMENT OF THE CORE

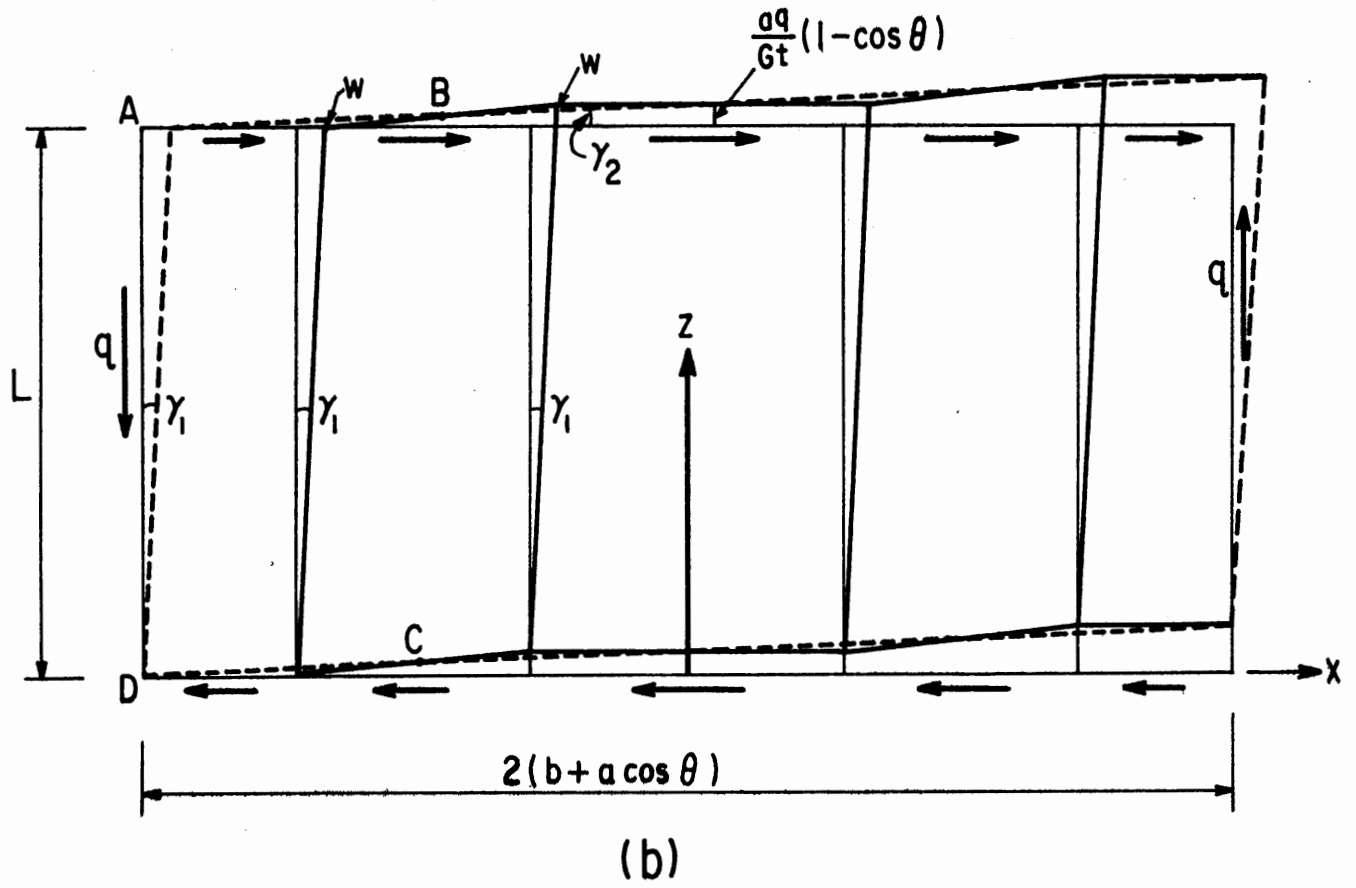
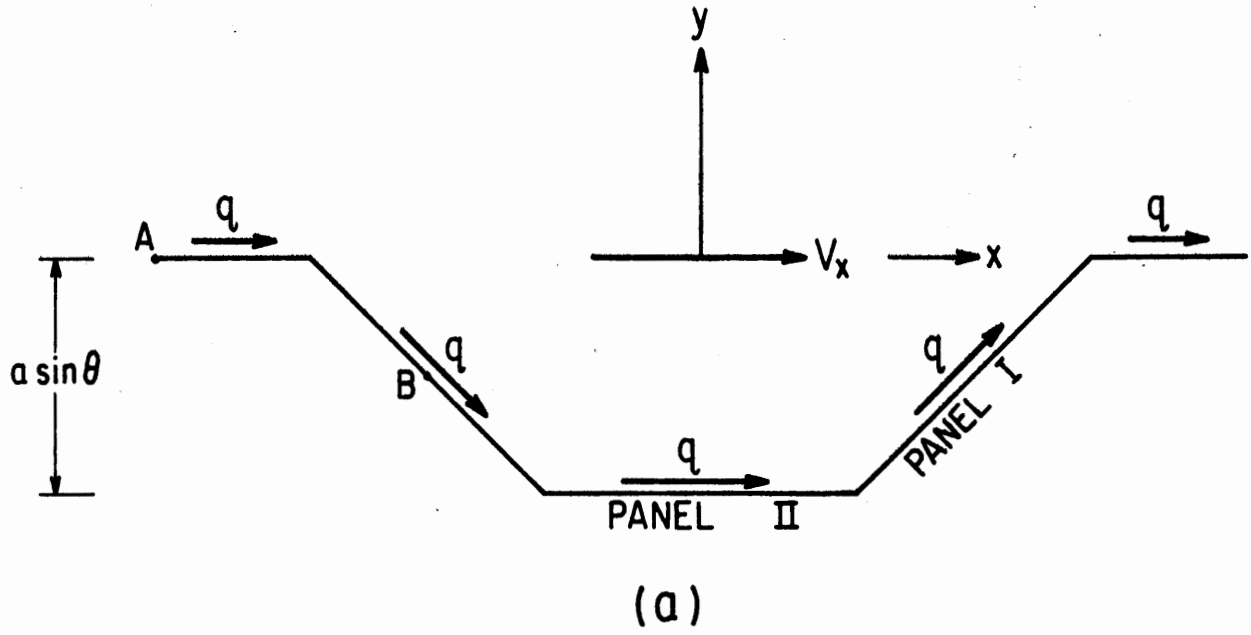


FIG. 3 SHEAR STRAINS IN CORE ELEMENT

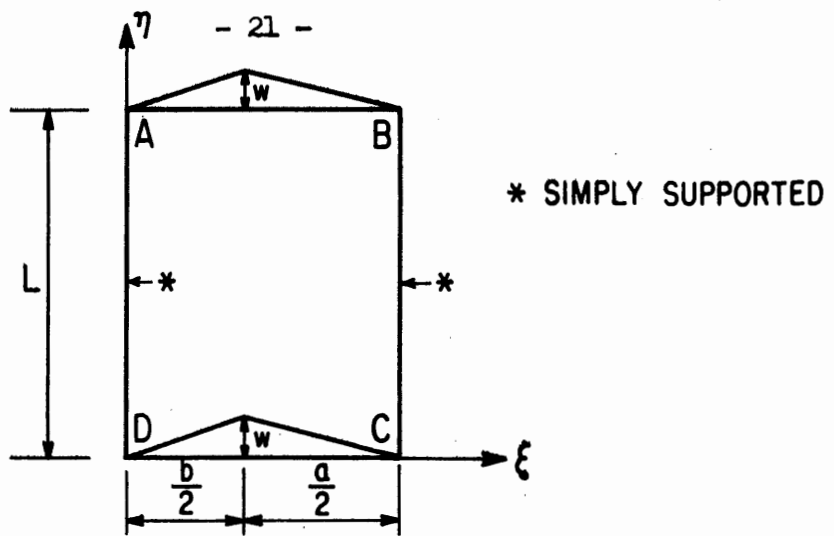


FIG. 4 TYPICAL ELEMENT ABCD

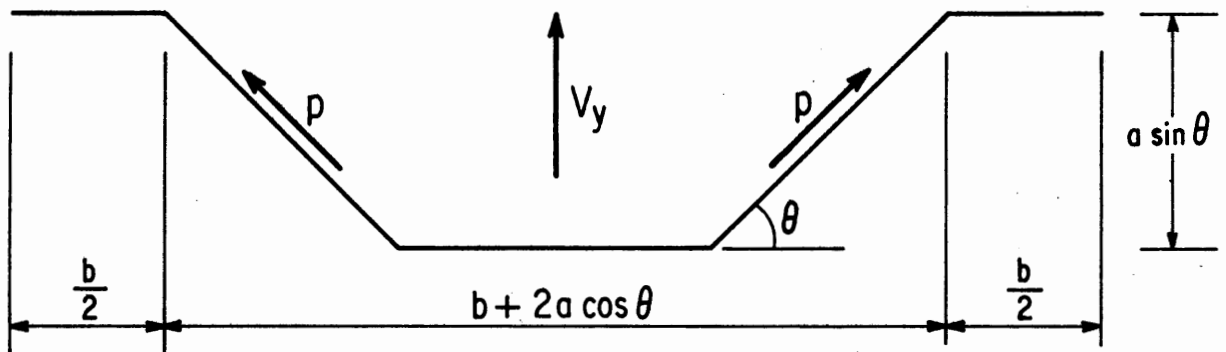


FIG. 5 PLAN VIEW OF TYPICAL ELEMENT OF THE CORE

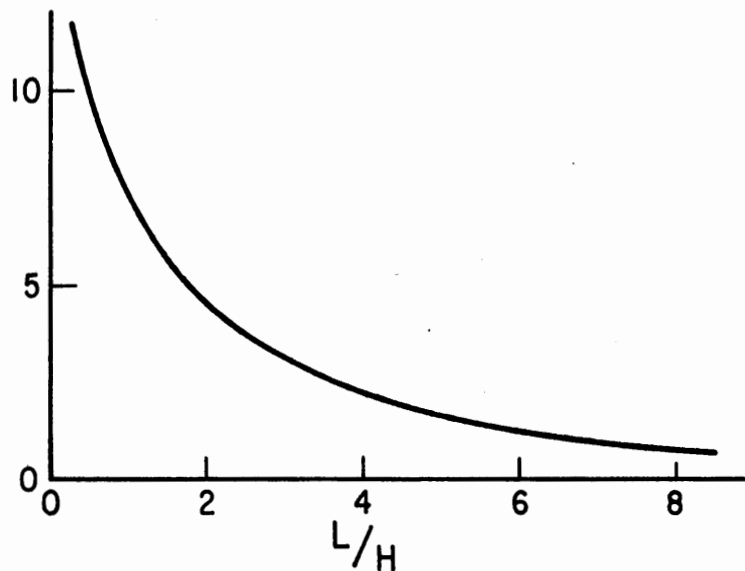


FIG. 6 PERCENTAGE INCREASE OF THE EFFECTIVE SHEAR MODULUS RATIO G_c/G DUE TO THE PREVENTION OF WARPAGE vs. L/H

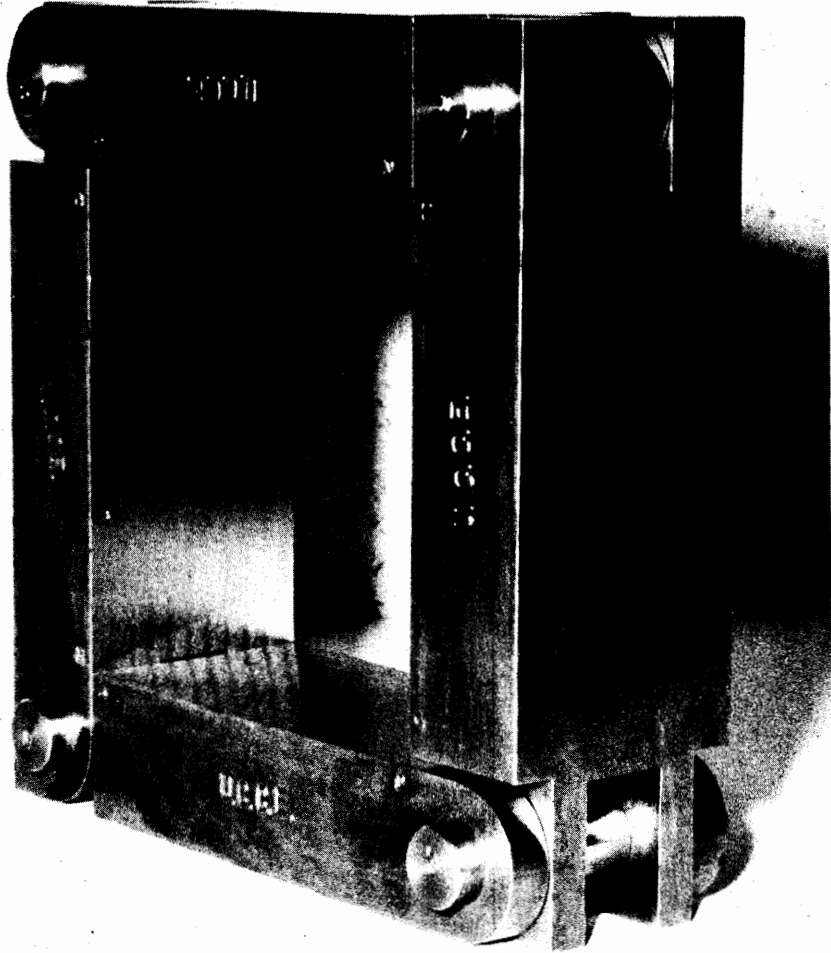


FIG. 7 TEST FRAME

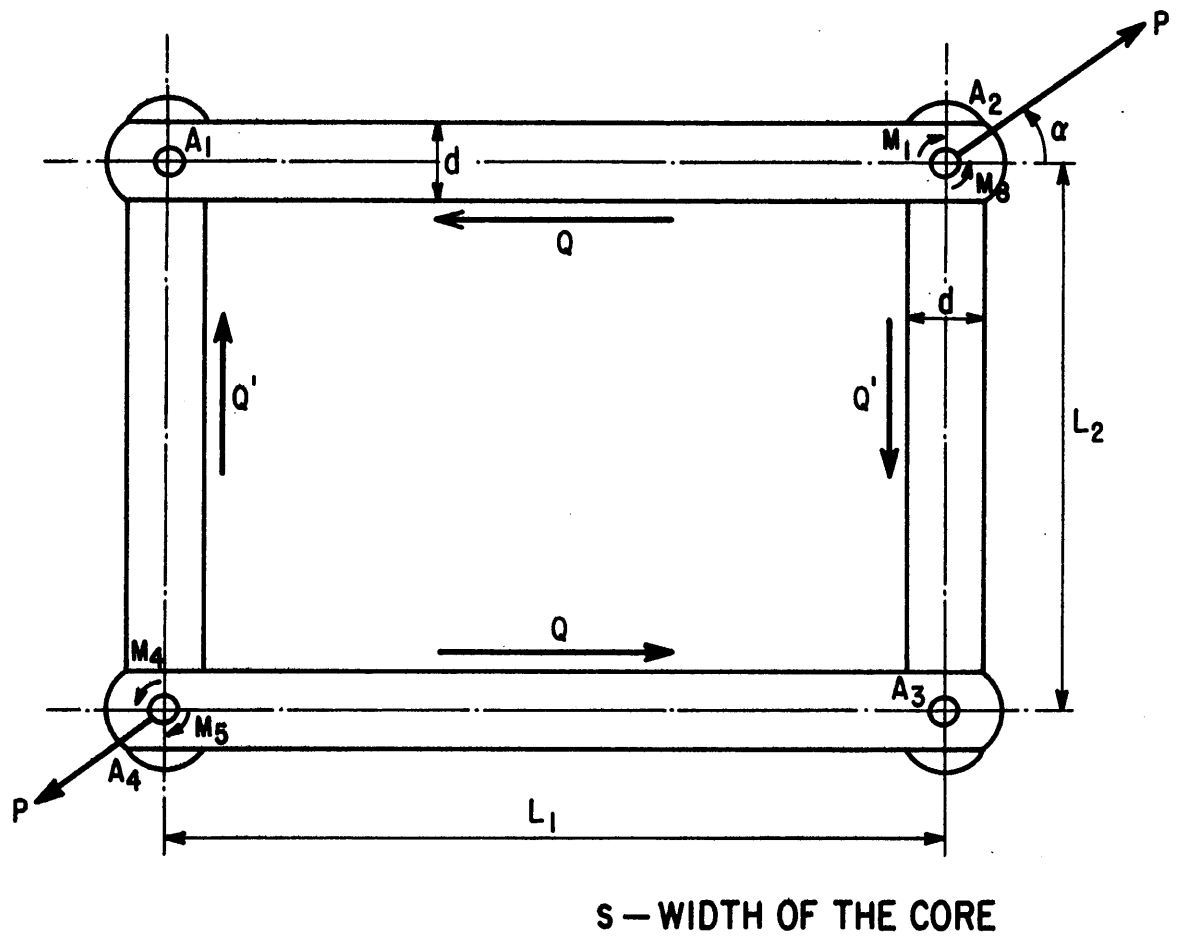


FIG. 8 SHEAR LOADING FRAME